Journal of Sound and Vibration (2001) **248**(4), 695–724
doi:10.1006/jsvi.2001.3811, available online at http://www.idealibrary.com on IDEAL®

MULTI-MODE TRIMMING OF IMPERFECT RINGS

A. K. Rourke, S. McWilliam and C. H. J. Fox

School of Mechanical, Materials, Manufacturing Engineering and Management, University of Nottingham, University Park, Nottingham NG7 2RD, England.
E-mail: stewart.mcwilliam@nottingham.ac.uk

(*Received* 10 *October* 2000, *and in final form* 12 *May* 2001)

This paper proposes a method for trimming the natural frequencies of an imperfect ring to simultaneously eliminate certain of the frequency splits present. Initially, the effect of the addition of a number of imperfection masses on a perfect ring is considered. This is achieved by using a Rayleigh–Ritz approach in which it is assumed that the mode shapes are identical to those of a perfect ring. By considering the inverse (the so-called trimming) problem it is deduced that it is possible to trim N pairs of modes simultaneously by removing (a minimum of) N trimming masses at particular locations around the ring. To calculate the trimming mass locations, it is necessary to solve N non-linear algebraic equations. Once this has been achieved, the magnitude of the trimming masses can be calculated easily. For the special case of trimming a single pair of modes, analytic solutions for the magnitude and position of the single required trimming mass are available. To trim two pairs of modes, it is shown that a simple analytic relationship exists between the angular positions of the two required trimming masses and that the magnitude of these masses can be obtained easily. To trim more pairs of modes, numerical techniques are required and for this purpose a numerical procedure is proposed. Validation of the derived analytic results and the proposed numerical procedure is achieved by studying a number of theoretical examples.

1. INTRODUCTION

In a perfectly axisymmetric ring, the vibration modes for a given nodal configuration occur in degenerate pairs that have equal natural frequencies, are spatially orthogonal and have indeterminate angular position. In reality, imperfections due to dimensional variations and material non-uniformity exist which give rise to small frequency splits, fixing the positions of the modes relative to the ring. The influence of such imperfections is of particular importance in the manufacture of gyroscopic rate sensors that are based on the vibration of a ring-shaped resonator [1]. In such applications, it is often necessary to reduce the frequency splits to the order of 0·01% to maintain strong resonant coupling between a pair of given modes. This paper deals with the reduction and possible elimination of small frequency splits that occur in rings, or other nominally axisymmetric structures, between pairs of modes of vibration with the same harmonic number.

The literature contains a variety of papers analyzing the influence of particular types of imperfection on the vibration characteristics of axisymmetric structures. One of the first studies was performed by Tobias [2] who gave a good description of the qualitative effects of imperfection. Other works include those by Charnley and Perrin, who investigated the addition of regularly spaced point masses to a circular ring using group theory [3] and a perturbation analysis [4]. Laura *et al.* [5] considered the effect of circumferential variation in the wall thickness of a ring on axisymmetric modes using both a Rayleigh–Ritz

0022-460X/01/490695 + 30 $35.00/0

and a finite element analysis whilst Tonin and Bies [6] considered the influence of circumferential variation in the wall thickness of an eccentric cylinder using a Rayleigh–Ritz analysis. This approach is based on the assumption that the imperfections are small, such that the mode shapes are unchanged by the presence of any imperfection, and has the advantage over other methods that relatively simple expressions for the natural frequencies and mode orientations can be obtained. This is especially the case for initially perfect circular rings with attached masses and springs as shown by Fox [7, 8]. The Rayleigh–Ritz approach has been used recently by Hwang *et al.* [9–11] to consider general profile variations of a ring, and by Eley *et al.* [12] to consider the influence of anisotropy on the vibration of circular crystalline silicon rings.

By introducing the concept of the "equivalent imperfection mass", Fox [7] showed that it is possible to consider the inverse (trimming) problem. This consisted of determining the size and location of the (single) mass that should be added to (or removed from) an initially imperfect ring to make the frequencies of a particular pair of modes the same. Thus, it was found that the addition of an appropriate single "trimming" mass at a particular position on the ring will eliminate the frequency split between one pair of $n\theta$ modes of the ring and remove the spatial orientation determinacy, where n is the number of nodal diameters of the mode. For many practical applications, the proposed trimming procedure is extremely useful. However, the method is restricted to the trimming of *one* pair of modes and is unlikely to simultaneously eliminate the frequency splits associated with other pairs of modes. Given that future developments in sensor technology may depend on the ability to trim more than one pair of modes at the same time, there is a need to consider the theoretical feasibility of simultaneously trimming a number of pairs of in-plane modes of an imperfect ring. This forms the motivation for the current work.

The principal aim of this paper is to report the results of an investigation that extends and generalizes the procedure and results given by Fox [7] to the simultaneous trimming of more than one pair of modes using more than one trimming mass. A general method for simultaneously trimming N pairs of modes using N trimming masses is outlined in section 2. Following this, the proposed method is applied to the special cases of single- and dual-mode trimming in sections 3 and 4, before the general multi-mode case is considered in section 5. Numerical examples demonstrating the developed methods are presented throughout.

2. THE TRIMMING PROBLEM

Consider an imperfect ring for which the natural frequencies of the pair of orthogonal modes having n nodal diameters are ω_{n1} and ω_{n2}. Here it is assumed that the radial (w) and tangential displacements (u) of the ring in these four modes are given by

$$\begin{aligned} w_{n1} &= W_{n1} \cos n(\phi - \psi_{n1}) \exp(\mathrm{i}\omega_{n1} t), \quad u_{n1} = U_{n1} \sin n(\phi - \psi_{n1}) \exp(\mathrm{i}\omega_{n1} t), \\ w_{n2} &= W_{n2} \cos n(\phi - \psi_{n2}) \exp(\mathrm{i}\omega_{n2} t), \quad u_{n2} = U_{n2} \sin n(\phi - \psi_{n2}) \exp(\mathrm{i}\omega_{n2} t), \end{aligned} \tag{1–4}$$

where the orientations $\psi_{n1} = \psi_{n2} - \pi/2n$. The assumption that the mode shapes are identical to those of a perfect ring adopted in these equations is reasonable provided that the degree of imperfection is sufficiently small. This assumption is tested in Appendix A using a Rayleigh–Ritz procedure.

Having made this assumption, the initial problem is to calculate the magnitudes and the angular positions of masses which, when added to a perfect ring, would produce the described "imperfect" natural frequencies and mode positions (see Figure 1). The effect of additional masses and springs on the natural frequencies and mode positions of a ring has

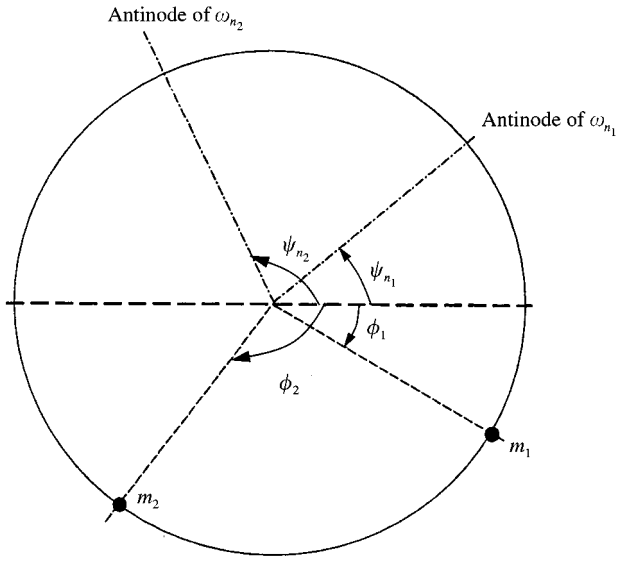

Figure 1. The imperfection masses and the generated imperfections.

been investigated previously by Fox [7]. In this work, a Rayleigh–Ritz approach was used to determine analytic expressions for the split natural frequencies in terms of the orientations and magnitudes of the added masses, radial springs and torsional springs. The orientation, ψ_n, of a specific $n\theta$ mode and its split frequencies, ω_{n1} and ω_{n2}, were found to be

$$\tan 2n\,\psi_n = \frac{\sum_i e_{in}(1-\alpha_n^2)\sin 2n\phi_i + \sum_j e_{jn}\alpha_n^2 \sin 2n\phi_j - \sum_k e_{kn}n^2\alpha_n^2 \sin 2n\phi_k}{\sum_i e_{in}(1-\alpha_n^2)\cos 2n\phi_i + \sum_j e_{jn}\alpha_n^2 \cos 2n\phi_j - \sum_k e_{kn}n^2\alpha_n^2 \cos 2n\phi_k}, \tag{5}$$

$$\omega_n^2 = \omega_{0n}^2 \frac{\{1 + \sum_j e_{jn}\alpha_n^2[1 + \cos 2n(\phi_j - \psi_n)] + \sum_j e_{kn}n^2\alpha_n^2[1 - \cos 2n(\phi_k - \psi_n)]\}}{\{1 + \sum_i e_{in}[(1+\alpha_n^2) - (1-\alpha_n^2)\cos 2n(\phi_i - \psi_n)]\}}, \tag{6}$$

in which $e_{in} = m_i/4T_{0n}$, $e_{jn} = K_{rj}/4S_{0n}$, $e_{kn} = K_{tk}/4R^2S_{0n}$ and R is the mean radius of the ring. m_i and ϕ_i denote the magnitude and angular co-ordinate of the ith added mass, K_{rj} and ϕ_j denote the stiffness and angular co-ordinate of the jth radial spring and K_{tk} and ϕ_k denote the stiffness and angular co-ordinate of the kth torsional spring. ω_{0n} is the natural frequency of the original perfect ring and α_n is the amplitude ratio W/U. The values for ω_{0n} and α_n have been calculated using the Rayleigh–Ritz method and Flügge's strain–displacement relations and can be seen in Appendix B.

Although the imperfections in a real ring may be introduced by both the mass and stiffness of its supports, such as internal legs, the aim of this method is to eliminate the imperfections by the removal or addition of mass to the ring. Thus, the effect of the radial and torsional springs can be neglected for this analysis. However, this does not invalidate the method for use on imperfections that have been introduced by a combination of masses and springs, as will be shown later by a numerical example.

By neglecting the effect of the springs, equations (5) and (6) can be simplified by setting e_{jn} and e_{kn} equal to zero. Also, as can be seen from equation (B8), it is possible to substitute a value for T_{0n} into e_{in}, which is that $T_{0n} = RhL\rho\pi(1+\alpha_n^2)/2 = M_0(1+\alpha_n^2)/4$, where M_0 is

the mass of the perfect ring. Thus, taking the mode orientations $\psi_n = \psi_{n1}$, equations (5) and (6) become

$$\tan 2n\psi_n = \frac{\sum_i m_i \sin 2n\phi_i}{\sum_i m_i \cos 2n\phi_i}. \tag{7}$$

$$\omega_{n1}^2 = \omega_{0n}^2 \left(\frac{1 + \alpha_n^2}{(1 + \alpha_n^2) + \sum_i m_i[(1 + \alpha_n^2) - (1 - \alpha_n^2) \cos 2n(\phi_i - \psi_n)]/M_0} \right), \tag{8}$$

$$\omega_{n2}^2 = \omega_{0n}^2 \left(\frac{1 + \alpha_n^2}{(1 + \alpha_n^2) + \sum_i m_i[(1 + \alpha_n^2) + (1 - \alpha_n^2) \cos 2n(\phi_i - \psi_n)]/M_0} \right). \tag{9}$$

Equations (7)–(9) provide a means of determining the frequency splits and mode orientations resulting from the addition of imperfection masses at particular locations to an initially perfect ring. In what follows, the inverse (trimming) problem is considered in which the aim is to determine the magnitude and angular location of masses that need to be removed from the ring in order to eliminate splits between particular pairs of natural frequencies. For this purpose, it is convenient to express the mass of the perfect ring in terms of the mass of the imperfect ring M, which will be known at the outset of the trimming analysis, and the added masses, i.e.,

$$M_0 = M - \sum_i m_i. \tag{10}$$

Substituting equation (10) into equations (8) and (9) yields:

$$\omega_{n1}^2 = \omega_{0n}^2 \left(\frac{(1 + \alpha_n^2)(M - \sum_i m_i)}{M(1 + \alpha_n^2) - (1 - \alpha_n^2) \sum_i m_i \cos 2n(\phi_i - \psi_n)]} \right), \tag{11}$$

$$\omega_{n2}^2 = \omega_{0n}^2 \left(\frac{(1 + \alpha_n^2)(M - \sum_i m_i)}{M(1 + \alpha_n^2) + (1 - \alpha_n^2) \sum_i m_i \cos 2n(\phi_i - \psi_n)]} \right). \tag{12}$$

These equations relate the natural frequencies of the imperfect ring to the trimmed natural frequency ω_{0n}. Given that ω_{0n} will not be known at the outset of the trimming analysis, it is necessary to eliminate this term between equations (11) and (12). This can be achieved easily by dividing the two equations. Following this procedure, it can be shown that the following relationship is obtained:

$$\sum_i m_i \cos 2n(\phi_i - \psi_n) = M\lambda_n, \tag{13}$$

where

$$\lambda_n = \frac{(\omega_{n1}^2 - \omega_{n2}^2)(1 + \alpha_n^2)}{(\omega_{n1}^2 + \omega_{n2}^2)(1 - \alpha_n^2)}. \tag{14}$$

Thus, to trim the imperfect ring it is necessary to determine the magnitude (m_i) and locations (ϕ_i) of the trimming masses that satisfy both equations (7) and (13) for all of the modes considered. Before discussing the solution of this problem, it is worthwhile noting that once the trimming masses have been calculated it is a simple task to calculate the trimmed natural frequencies using either equation (11) or (12), or a combination of both.

Inspection of equations (7) and (13) indicates that the terms associated with the magnitude of the trimming masses, m_i, are linear, while those related to the angular orientation of the masses, ϕ_i, involve non-linear, trigonometric functions. To facilitate the solution of these equations, it is sensible to maintain the linear aspects of these equations and, with this in mind, equation (7) is re-written as follows:

$$\sum_i m_i \sin 2n(\phi_i - \psi_n) = 0, \tag{15}$$

where standard trigonometric identities have been used in the formation of this equation.

So far, the number of pairs of modes to be trimmed has not been discussed. In what follows, it is assumed that it is required to trim N pairs of modes using N trimming masses. Thus, denoting the N pairs of modes by $n_1, n_2, \ldots, n_N$ (where $n_j \neq n_k$ when $j \neq k$), the trimming problem reduces to finding values for m_i and ϕ_i that satisfy the following two sets of equations:

$$\sum_{i=1}^{N} m_i \sin 2n_j(\phi_i - \psi_{n_j}) = 0, \tag{16}$$

$$\sum_{i=1}^{N} m_i \cos 2n_j(\phi_i - \psi_{n_j}) = M\lambda_{n_j}, \tag{17}$$

where $j = 1, 2, \ldots, N$.

For the purposes of analysis, it is convenient to express equations (16) and (17) in matrix notation as follows:

$$\mathbf{Am} = \mathbf{0}, \quad \mathbf{Bm} = \mathbf{c}, \tag{18, 19}$$

where $\mathbf{A}$ is a square matrix whose jkth element is $\sin 2n_j(\phi_k - \psi_{n_j})$, $\mathbf{B}$ is a square matrix whose jkth element is $\cos 2n_j(\phi_k - \psi_{n_j})$, $\mathbf{m}$ is a vector whose kth element is m_k, and $\mathbf{c}$ is a vector whose kth element is $M\lambda_{n_k}$.

In general, solutions to equations (18) and (19) enable the mass and angular positions of the trimming masses to be obtained. Given that matrices $\mathbf{A}$ and $\mathbf{B}$ are dependent upon the angular locations only and vector $\mathbf{m}$ contains the magnitude of the trimming masses only, it may be deduced that once the angular locations are known, it is a simple task to solve equation (19) (say) to calculate the magnitude of the trimming masses. Thus, the main problem that needs addressing is to calculate the angular locations of the trimming masses. This is best achieved by eliminating the mass vector $\mathbf{m}$ between equations (18) and (19). This gives

$$\mathbf{AB}^{-1}\mathbf{c} = \mathbf{0}. \tag{20}$$

Equation (20) provides what appears to be a relatively simple relationship between the angular positions of the trimming masses. In general, numerical techniques must be used to determine solutions to these equations. However, in some situations it will be shown that it is possible to deduce simple analytical relationships between the angular positions of the trimming masses that aid the solution of this equation. This is achieved by noting that all solutions to equation (20) must satisfy the non-trivial solution to equation (18):

$$\det(\mathbf{A}) = 0. \tag{21}$$

This determinant equation relates the angular orientations of the masses, and is independent of the magnitude of the trimming masses. However, it is worthwhile noting that not all solutions to equation (21) are solutions to equation (20), even though all solutions to equation (20) are solutions to equation (21). The equations developed in this section will be used in subsequent sections to trim single-, dual- and multi-frequency mode pairs of an imperfect ring.

3. SINGLE MODE FREQUENCY TRIMMING

Consider the situation when $N = 1$. In this special case, equation (20) yields

$$M\lambda_n \tan 2n(\phi - \psi_n) = 0, \tag{22}$$

indicating that the trimming mass must be located at $\phi = \psi_n, \psi_n \pm \pi/2n$.

Before considering the magnitude of the trimming mass, it is worthwhile noting that for the case considered, equation (21) yields

$$\sin 2n(\phi - \psi_n) = 0, \tag{23}$$

which possesses identical solutions to equation (22). Thus, in this case the solution to the determinant equation is always a solution to the trimming problem.

Using equation (19) it is found that the magnitude of the trimming mass is

$$m = M\lambda_n = \frac{M(\omega_{n1}^2 - \omega_{n2}^2)(1 + \alpha_n^2)}{(\omega_{n1}^2 + \omega_{n2}^2)(1 - \alpha_n^2)} \quad \text{when } \phi = \psi_n \tag{24}$$

and

$$m = -M\lambda_n = \frac{-M(\omega_{n1}^2 - \omega_{n2}^2)(1 + \alpha_n^2)}{(\omega_{n1}^2 + \omega_{n2}^2)(1 - \alpha_n^2)} \quad \text{when } \phi = \psi_n \pm \frac{\pi}{2n}. \tag{25}$$

Equation (24) corresponds to removing mass m from the ring, while equation (25) corresponds to adding an identical amount but at a different location. These results agree with those published by Fox [7]. Given that these results were compared in some detail with the previous work in reference [7], the above results are not considered any further here.

4. DUAL-MODE FREQUENCY TRIMMING

Consider the special situation when $N = 2$. In this case:

$$\mathbf{A} = \begin{pmatrix} \sin 2n_1(\phi_1 - \psi_{n_1}) & \sin 2n_1(\phi_2 - \psi_{n_1}) \\ \sin 2n_2(\phi_1 - \psi_{n_2}) & \sin 2n_2(\phi_2 - \psi_{n_2}) \end{pmatrix},$$

$$\mathbf{B} = \begin{pmatrix} \cos 2n_1(\phi_1 - \psi_{n_1}) & \cos 2n_1(\phi_2 - \psi_{n_1}) \\ \cos 2n_2(\phi_1 - \psi_{n_2}) & \cos 2n_2(\phi_2 - \psi_{n_2}) \end{pmatrix} \tag{26, 27}$$

and

$$\mathbf{c} = \begin{pmatrix} M\lambda_{n_1} \\ M\lambda_{n_2} \end{pmatrix}. \tag{28}$$

Although the solution of equation (20) forms the most direct route to obtaining solutions to the trimming problem, it is convenient here to consider the form of equation (21) first. Substituting matrix **A** into equation (21) it may be shown (see Appendix C) that the following relationship must be satisfied:

$$\begin{aligned}&\tan((n_1+n_2)\,\phi_1 - n_1\psi_{n_1} - n_2\psi_{n_2})\tan((n_1-n_2)\,\phi_2 - n_1\psi_{n_1} + n_2\psi_{n_2})\\ &\quad = \tan((n_1+n_2)\phi_2 - n_1\psi_{n_1} - n_2\psi_{n_2})\tan((n_1-n_2)\phi_1 - n_1\psi_{n_1} + n_2\psi_{n_2}).\end{aligned} \tag{29}$$

As mentioned earlier, this result is independent of the magnitude of the masses and therefore provides a relatively simple relationship governing the possible positions of the trimming masses. It should be re-called though that not all solutions to equation (29) are solutions to the trimming problem.

A trivial solution to equation (29) is obtained when $\phi_1 = \phi_2$. Substituting these angular positions into matrix **B** yields a matrix whose inverse is ill defined, corresponding to trimming masses of infinite magnitude. The invalidity of this solution provides some justification for the reasoning that in general a single trimming mass (i.e., two masses at the same location) cannot be used to trim two pairs of modes simultaneously.

To proceed, it is necessary to consider the solution of equation (20). This process is aided by making use of equation (21), both directly and in its modified form of equation (29). It may be shown (see Appendix D) that this manipulation re-arranges equation (20) into the following pair of simultaneous equations:

$$\begin{aligned}&\left(\tan((n_1+n_2)\,\phi_1 - n_1\psi_{n_1} - n_2\psi_{n_2})\tan((n_2-n_1)\,\phi_2 - n_2\psi_{n_2} + n_1\psi_{n_1}) - \frac{\lambda_{n_2}-\lambda_{n_1}}{\lambda_{n_2}+\lambda_{n_1}}\right)\\ &\quad\times(\tan((n_1+n_2)\phi_1 - n_1\psi_{n_1} - n_2\psi_{n_2}) - \tan((n_1+n_2)\phi_2 - n_1\psi_{n_1} - n_2\psi_{n_2})) = 0,\end{aligned} \tag{30}$$

$$\begin{aligned}&\left(\tan((n_1+n_2)\,\phi_1 - n_1\psi_{n_1} - n_2\psi_{n_2})\tan((n_2-n_1)\,\phi_2 - n_2\psi_{n_2} + n_1\psi_{n_1}) - \frac{\lambda_{n_2}-\lambda_{n_1}}{\lambda_{n_2}+\lambda_{n_1}}\right)\\ &\quad\times(\tan((n_2-n_1)\phi_1 - n_2\psi_{n_2} + n_1\psi_{n_1}) - \tan((n_2-n_1)\phi_2 - n_2\psi_{n_2} + n_1\psi_{n_1})) = 0.\end{aligned} \tag{31}$$

It can be seen that equations (30) and (31) contain a common factor and so the solutions to both equations can be found when

$$\tan((n_1+n_2)\phi_1 - n_1\psi_{n_1} - n_2\psi_{n_2})\tan((n_2-n_1)\phi_2 - n_2\psi_{n_2} + n_1\psi_{n_1}) = \frac{\lambda_{n_2}-\lambda_{n_1}}{\lambda_{n_2}+\lambda_{n_1}}. \tag{32}$$

Valid angular locations can be obtained by solving equation (32) and an equivalent form of this equation generated by interchanging ϕ_1 and ϕ_2; this interchange is permissible due to the arbitrary choice of the angular positions of the trimming masses. Thus, the angular positions of the trimming masses can be found by solving the following two simultaneous equations:

$$\tan((n_1+n_2)(\phi_1+\delta_1))\tan((n_2-n_1)(\phi_2+\delta_2)) = \frac{\lambda_{n_2}-\lambda_{n_1}}{\lambda_{n_2}+\lambda_{n_1}}, \tag{33}$$

$$\tan((n_1+n_2)(\phi_2+\delta_1))\tan((n_2-n_1)(\phi_1+\delta_2)) = \frac{\lambda_{n_2}-\lambda_{n_1}}{\lambda_{n_2}+\lambda_{n_1}}, \tag{34}$$

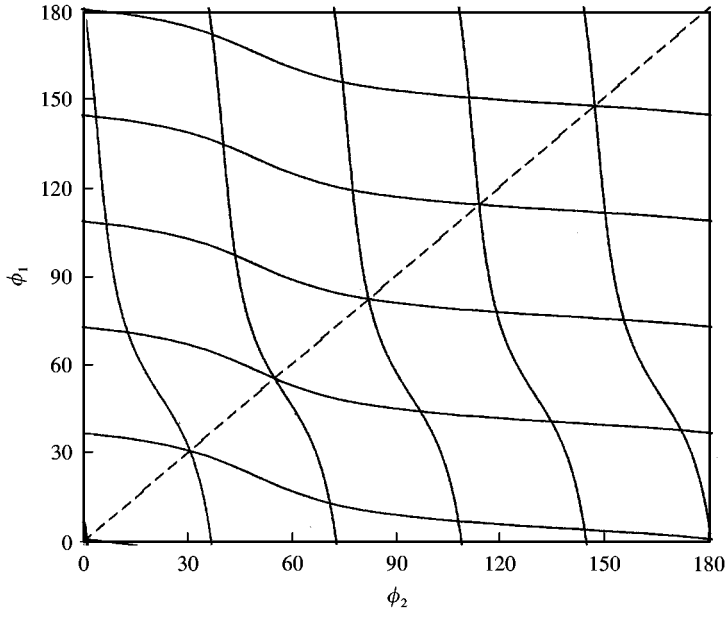

Figure 2. Graphical representations of equations (33) and (34) for ($n_1 = 2$, $n_2 = 3$) for the three imperfection masses example.

where

$$\delta_1 = -\left(\frac{n_1\psi_{n_1} + n_2\psi_{n_2}}{n_1 + n_2}\right), \quad \delta_2 = \frac{n_1\psi_{n_1} - n_2\psi_{n_2}}{n_2 - n_1}. \tag{35, 36}$$

Valid solutions to equations (33) and (34) can be found graphically by considering the intersection of the curves produced by these equations. An example that demonstrates this process can be seen in Figure 2. This figure shows plots of equations (33) and (34) for the third example considered in the numerical examples section for ($n_1 = 2$, $n_2 = 3$). The points where the curves intersect provide a clear indication of the angular locations at which trimming masses could be placed. Of course, in a practical solution procedure, it is necessary to use numerical "search" techniques to calculate the precise intersection points and the accuracy to which these solutions are obtained governs the accuracy of the final trimming solution.

In addition, it is worthwhile noting that equations (33) and (34) contain members of the set of solutions $\phi_1 = \phi_2$ which produce ill-defined trimming masses, as has already been indicated. These solutions are neglected within the solution procedure.

A translation of either ϕ_1 or ϕ_2 (or both) by $\pm 180^\circ$ will have no effect on equations (33) and (34) due to the symmetry of the trigonometric identity. In addition, this translation will have no effect on the original equations (11)–(13). For these reasons, it is only necessary to investigate angular positions in the range $0 < \phi_i < 180^\circ$ to find all possible solutions.

By considering these factors, it is possible to predict the number of unique angular solutions that can be obtained for specific values of ϕ_1 and ϕ_2 that exist in the range $0 < \phi_i < 180^\circ$. There will occasionally be a difference between the physically achievable number of solutions and the number predicted, which will be due to the shape of equations (33) and (34). In general, though, it may be shown [13] that there will be a maximum of

$(n_1 + n_2)(n_1 + n_2 - r)/2r^2$ unique angular solutions, where r is the highest common factor of n_1 and n_2. Thus, it is possible to predict how many unique solutions can be obtained.

Once the angular locations of the trimming masses have been identified, the magnitude of the trimming masses can be calculated. In general, it is possible to calculate the trimming masses directly from equation (19). However, there is one limitation to this. It is possible that the frequency splits that are to be eliminated from the imperfect ring are equivalent to the addition of a single imperfection mass and not a pair of distinct imperfection masses, as has been assumed. In this case, the inverse of matrix **B** may be indeterminable, meaning that the trimming masses are poorly defined. For this reason, an alternative method of calculating the trimming masses is required that satisfies this case. This is described next.

Using equation (18) the magnitude of mass m_2 can be found in terms of mass m_1 and, by substituting this relationship into equation (13), the following pair of trimming mass equations can be obtained:

$$m_1 = M\lambda_{n_1} \frac{\sin 2n_1(\phi_2 - \psi_{n_1})}{\sin 2n_1(\phi_2 - \phi_1)}, \tag{37}$$

$$m_2 = M\lambda_{n_1} \frac{\sin 2n_1(\phi_1 - \psi_{n_1})}{\sin 2n_1(\phi_1 - \phi_2)}. \tag{38}$$

For the troublesome case of a single imperfection mass, a possible solution is that $\phi_1 = \psi_{n_1}$ and ϕ_2 is arbitrary. Substituting these values of ϕ_1 and ϕ_2 into equations (37) and (38) produces a zero trimming mass for m_2 and a mass of $M\lambda_{n_1}$ for m_1. These results are in complete agreement with the results obtained for single-mode frequency trimming, as illustrated by equation (24). Equations (37) and (38) have general applicability to all dual-mode problems and are used in the numerical examples presented below.

The validity of the results presented in this section will be illustrated next for a number of imperfect rings. The examples investigated are identical to those considered previously by Fox [7] and consist of trimming two pairs of modes of a perfect ring to which have been attached either:

(1) one imperfection mass;
(2) one imperfection mass and one radial spring;
(3) three imperfection masses.

The dimensions of the perfect ring are included in Appendix E and the sizes of the imperfection masses and the radial springs are specified as each example is considered.

The first step in each example is to calculate the original frequency splits. For cases (1) and (3), which involve added masses only, this is achieved easily using equations (7)–(9). However, for case (2) it is necessary to use a more complete form of these equations, taking into account the effect of the spring. In this case, the original frequency splits and mode orientations can be found from equations (5) and (6) by setting e_{kn} equal to zero and replacing j by p:

$$\tan 2n\psi_n = \frac{(1 - \alpha_n^2)\sum_i m_i(\sin 2n\phi_i)/(M_0(1 + \alpha_n^2)) + \alpha_n^2 \sum_p e_{pn} \sin 2n\phi_p}{(1 - \alpha_n^2)\sum_i m_i(\cos 2n\phi_i)/(M_0(1 + \alpha_n^2)) + \alpha_n^2 \sum_p e_{pn} \cos 2n\phi_p}, \tag{39}$$

$$\omega_{n1}^2 = \omega_{0n}^2 \left(\frac{1 + \sum_p e_{pn}\alpha_n^2(1 + \cos 2n(\phi_p - \psi_n))}{1 + \sum_i m_i[(1 + \alpha_n^2) - (1 - \alpha_n^2)\cos 2n(\phi_i - \psi_n)]/(M_0(1 + \alpha_n^2))} \right), \tag{40}$$

$$\omega_{n2}^2 = \omega_{0n}^2 \left(\frac{1 + \sum_p e_{pn}\alpha_n^2(1 - \cos 2n(\phi_p - \psi_n))}{1 + \sum_i m_i[(1 + \alpha_n^2) + (1 - \alpha_n^2)\cos 2n(\phi_i - \psi_n)]/(M_0(1 + \alpha_n^2))} \right), \tag{41}$$

where e_{pn} is given by

$$e_{pn} = \frac{K_{rp} R(1 - v^2)}{2\pi E a[(n^2 - \alpha_n^2) + \beta(1 - n^2)^2 \alpha_n^2]} \tag{42}$$

and all other notations are defined in Appendix F.

Following the calculation of the initial frequency splits, it is necessary to consider the trimming masses necessary to correct for the imposed frequency splits for two different pairs of modes.

(1) *One imperfection mass.* Consider the addition of a single imperfection mass of mass 0·37 kg to the ring specified in Appendix E. For the purposes of analysis, it is convenient to locate the imperfection mass at the angular origin. As expected, it can be shown that the removal of this mass will eliminate all frequency splits. In addition to this solution, it will be shown that there is also a set of non-trivial solutions, which simultaneously eliminate the frequency splits in the modes with n_1 and n_2 nodal diameters. The case considered here is that of trimming the $n_1 = 2$ and $n_2 = 3$ modes simultaneously.

The solutions to this problem can be found analytically, obviating the need to use the proposed graphical method. This is possible due to the symmetry of the values of λ_n for the single mass case. It was shown in section 3 that the application of a single imperfection mass, m_1, at an angular position $\phi = 0$ will orientate all of the modes to the same angle such that $\psi_n = \phi$ and that by the substitution of these conditions into equations (11) and (12), the frequency splits are determined. By substituting the relevant frequency splits into equation (14) it can be shown that

$$\lambda_{n_1} = \lambda_{n_2} = m_1/(m_1 + M_0). \tag{43}$$

This relationship simplifies the pair of simultaneous equations (33) and (34) that need to be solved to obtain the locations of the trimming masses, giving

$$\tan((n_1 + n_2)\phi_1) \tan((n_2 - n_1)\phi_2) = 0, \tag{44}$$

$$\tan((n_1 + n_2)\phi_2) \tan((n_2 - n_1)\phi_1) = 0, \tag{45}$$

where $\delta_1 = \delta_2 = 0$ has been used since $\psi_n = 0$. These equations provide two sets of angular solutions, such that

$$(1)\ \phi_1 = \frac{k\pi}{n_2 + n_1}, \quad \phi_2 = \frac{l\pi}{n_2 + n_1}, \quad \text{where } k, l = -(n_2 + n_1), \ldots, -1, 0, 1, \ldots, (n_2 + n_1),$$

$$(2)\ \phi_1 = \frac{k\pi}{n_2 - n_1}, \quad \phi_2 = \frac{l\pi}{n_2 - n_1}, \quad \text{where } k, l = -(n_2 - n_1), \ldots, -1, 0, 1, \ldots, (n_2 - n_1)$$

when $n_2 > n_1$.

These angular locations are shown graphically in Figure 3. The masses that need to be attached at these angular positions are determined using equations (37) and (38).

The effect that the trimming masses have on the frequency splits for the $n = 2$, 3, 4 and 5 modes is recorded in Table 1. The frequencies shown in the first row of the table correspond to the original frequencies of the imperfect ring. One of each pair of frequencies is orientated such that it has a radial antinode at $\psi_n = 0$. The second row shows the trivial solution, in which ϕ_2 is irrelevant as there is no need to place a physical mass at that point. The other rows show all other solutions to equations (44) and (45). Only a single frequency

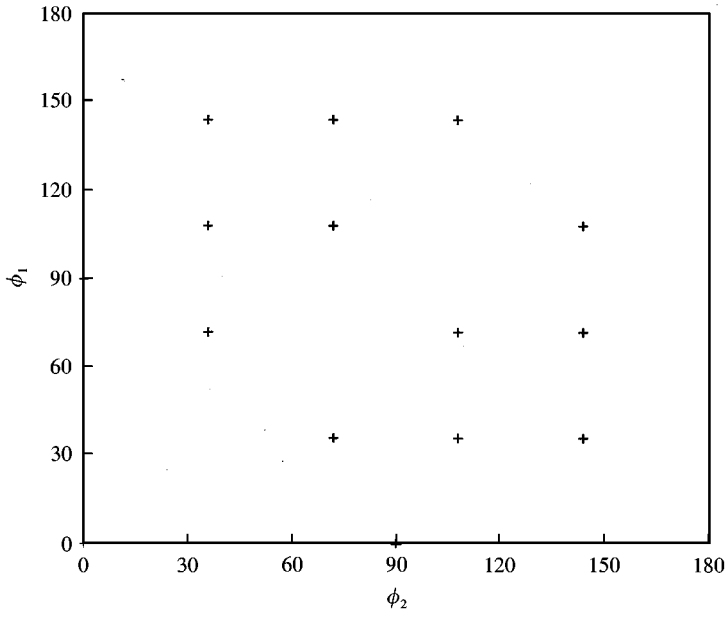

Figure 3. Solutions for ($n_1 = 2$, $n_2 = 3$) for the single imperfection mass example.

has been recorded for $n = 2$ and 3 as the procedure trims the pairs of unique frequencies into pairs of degenerate (Dg.) identical frequencies. For reasons already stated, the negative valued angular positions have not been included. As can be seen in Table 1, angular positions (ϕ_1, ϕ_2) and ($180 - \phi_1$, $180 - \phi_2$) produce the same trimming masses and trim the $n = 2$ and 3 frequency splits to the same natural frequency. This is a consequence of the symmetry of equations (37) and (38). In the general case, this will not be observed, as it is rare for both (ϕ_1, ϕ_2) and ($180 - \phi_1$, $180 - \phi_2$) to be solutions to the trimming problem.

The effect that the trimming masses have on the $n = 4$ and 5 modes of the ring is also shown in Table 1. Since the orientations of the modes do not necessarily remain at 0°, the specific orientations of the modes have been included. It can be seen that, with the exception of the removal of the original imperfection mass, the addition of the trimming masses do not eliminate the frequency splits in all modes shown. The ω_{n2} mode of the $n = 5$ modes is not greatly affected by the trimming masses as the masses are located at radial nodal positions. However, all other frequencies are significantly changed.

From the results presented it can be seen that, for the case considered, a pair of trimming masses can be used to eliminate the frequency splits of two pairs of modes, but that the effect on other modes cannot be controlled. Of course, in practise it is extremely unlikely that the frequency splits can be represented by a single imperfection mass. For this reason, it is necessary to consider some more complex imperfections.

(2) *One imperfection mass with one radial spring.* Consider an imperfect ring that can be represented by a perfect ring to which has been attached a single mass and a single radial spring. The reason for this investigation is that the previous example did not take into account a means by which the system can be supported. For instance, the ring used in a vibrating gyroscope is supported by a number of legs attached either in the form of internal spokes or external supports. These legs not only add stiffness to the ring but also alter the natural frequencies of the structure. To test fully the proposed method the influence of the stiffness of the supports is considered here.

TABLE 1

Trimming mass solutions for dual-mode trimming case (1)

Trimming masses				$n = 2$			$n = 3$			$n = 4$			$n = 5$		
ϕ_1 (deg)	m_1 (kg)	ϕ_2 (deg)	m_2 (kg)	ψ_n (deg)	ω_{n1} (Hz)	ω_{n2} (Hz)	ψ_n (deg)	ω_{n1} (Hz)	ω_{n2} (Hz)	ψ_n (deg)	ω_{n1} (Hz)	ω_{n2} (Hz)	ψ_n (deg)	ω_{n1} (Hz)	ω_{n2} (Hz)
—	—	—	—	0	35·390	36·417	0	99·638	103·51	0	190·69	198·88	0	308·09	321·95
0	− 0·370	N/A	0	Dg.	36·779		Dg.	104·02		Dg.	199·46	199·46	Dg.	322·57	322·57
36	0·599	72	0·370	Dg.	33·843		Dg.	95·723		− 9·0	176·32	191·73	0	277·81	320·35
36	0·370	108	− 0·229	Dg.	35·570		Dg.	100·60		− 4·5	184·57	202·48	0	303·05	321·72
36	0·229	144	0·229	Dg.	34·880		Dg.	98·655		0	184·18	194·57	0	292·62	321·19
72	− 0·599	108	− 0·599	Dg.	39·028		Dg.	110·39		0	194·86	233·72	0	364·14	323·97
72	− 0·229	144	0·370	Dg.	35·570		Dg.	100·60		4·5	184·57	202·48	0	303·05	321·72
108	0·370	144	0·599	Dg.	33·843		Dg.	95·723		9·0	176·32	191·73	0	277·81	320·35

Dg. indicates a degenerate pair of modes.

TABLE 2

Trimming mass solutions for dual-mode trimming case (2)

Trimming masses				$n = 2$			$n = 3$			$n = 4$			$n = 5$		
ϕ_1 (deg)	m_1 (kg)	ϕ_2 (deg)	m_2 (kg)	ψ_n (deg)	ω_{n1} (Hz)	ω_{n2} (Hz)	ψ_n (deg)	ω_{n1} (Hz)	ω_{n2} (Hz)	ψ_n (deg)	ω_{n1} (Hz)	ω_{n2} (Hz)	ψ_n (deg)	ω_{n1} (Hz)	ω_{n2} (Hz)
—	—	—	—	0	35·390	36·958	0·50	99·740	103·622	0	190·80	198·88	− 0·03	308·13	321·99
0·19	− 0·465	89·03	− 0·096	Dg.	37·530		Dg.	105·507		0·57	204·60	199·78	8·87	327·58	326·15
1·94	− 0·468	126·73	0·116	Dg.	36·997		Dg.	104·009		8·44	202·05	196·62	4·27	327·43	317·24
8·65	− 0·406	168·61	− 0·323	Dg.	37·977		Dg.	106·763		− 8·95	202·97	206·19	− 1·32	320·62	341·90
35·33	0·780	68·91	0·490	Dg.	33·512		Dg.	94·212		− 10·93	173·39	188·59	− 1·24	270·56	319·16
36·87	0·488	105·09	− 0·302	Dg.	35·723		Dg.	100·429		− 1·64	183·81	202·38	2·04	300·38	323·12
39·02	0·316	141·32	0·300	Dg.	34·793		Dg.	97·815		− 3·85	181·22	194·29	0·14	288·88	319·49
51·28	0·123	178·34	− 0·452	Dg.	36·939		Dg.	103·846		− 11·14	201·35	196·66	− 4·67	326·88	316·79
72·97	− 0·791	107·52	− 0·781	Dg.	40·473		Dg.	113·783		4·41	200·50	241·10	0·34	388·60	324·89
75·24	− 0·318	143·62	0·482	Dg.	35·773		Dg.	100·570		− 1·48	187·33	198·55	− 1·94	300·94	323·39
111·40	0·516	145·15	0·791	Dg.	33·445		Dg.	94·025		− 10·41	188·16	173·08	1·58	269·74	319·00

Dg. indicates a degenerate pair of modes.

Consider the addition of a single imperfection mass of mass 0·37 kg to the original perfect ring, which is being supported by a massless radial spring with a stiffness of 7400 N/m at an angle of 45° to the imperfection mass within the plane of the ring. This is a reasonable arrangement to introduce a degree of stiffness imperfection into the system although it may be argued that massless springs do not exist.

As with the single imperfection mass example, the first two modes will be trimmed and then the effect that this trimming has on the next two modes will be considered. The trimmed modes for the $n = 2$ and 3 case are recorded in Table 2 with the original untrimmed frequencies heading each of the columns. The effect that these trimming masses have on the $n = 4$ and 5 modes is also shown in Table 2. As in the previous example considered, it is observed that the frequency splits for these modes have not been eliminated.

A comparison of the solutions to this problem with the solutions to the single imperfection mass problem indicates only small differences between the angular positions of the trimming masses. These differences may be observed in Figure 4 and are due to the presence of the spring. On comparing Tables 1 and 2 it may be seen that although the masses are situated at similar locations, the trimming masses have increased significantly in magnitude in case (2).

The symmetry of the angular positions (ϕ_1, ϕ_2) and $(180 - \phi_1, 180 - \phi_2)$ observed in case (1) is approximately satisfied in case (2) (see Table 2). The small difference in angular solutions that was introduced by the radial spring means that there are no exact pairs of solutions (ϕ_1, ϕ_2) and $(180 - \phi_1, 180 - \phi_2)$. There are approximate pairs, however, and the required trimming masses and trimmed natural frequencies at these angular positions are comparable.

The procedure has been validated for the simultaneous trimming of two pairs of modes of an imperfect ring that can be represented by a perfect ring to which a single imperfection

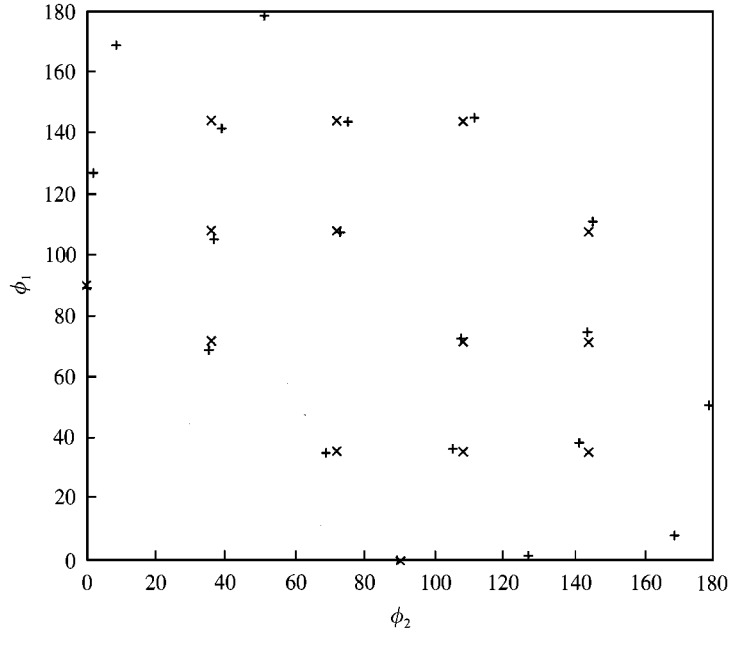

Figure 4. Comparison of the solutions for $(n_1 = 2, n_2 = 3)$ between the single imperfection mass example and the combined imperfection mass and spring example. +, spring and mass example; ×, single mass example.

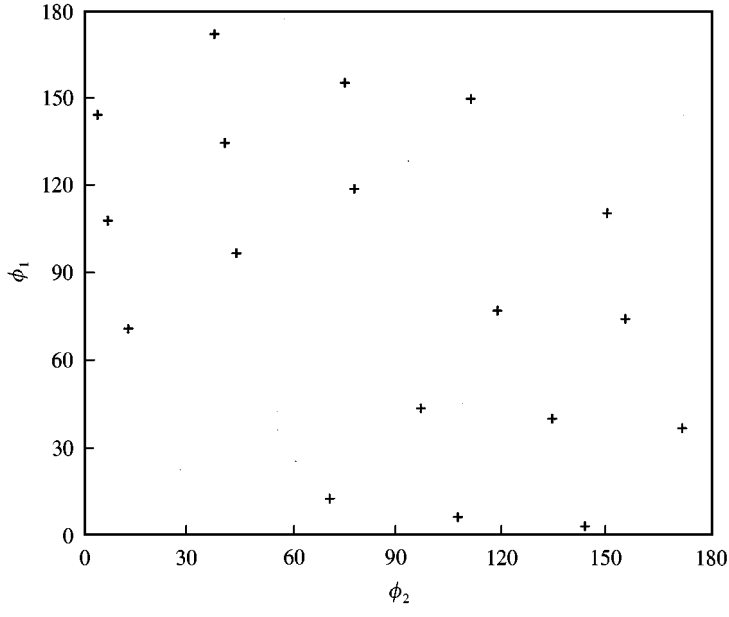

Figure 5. Solutions for ($n_1 = 2$, $n_2 = 3$) for the three imperfection masses example.

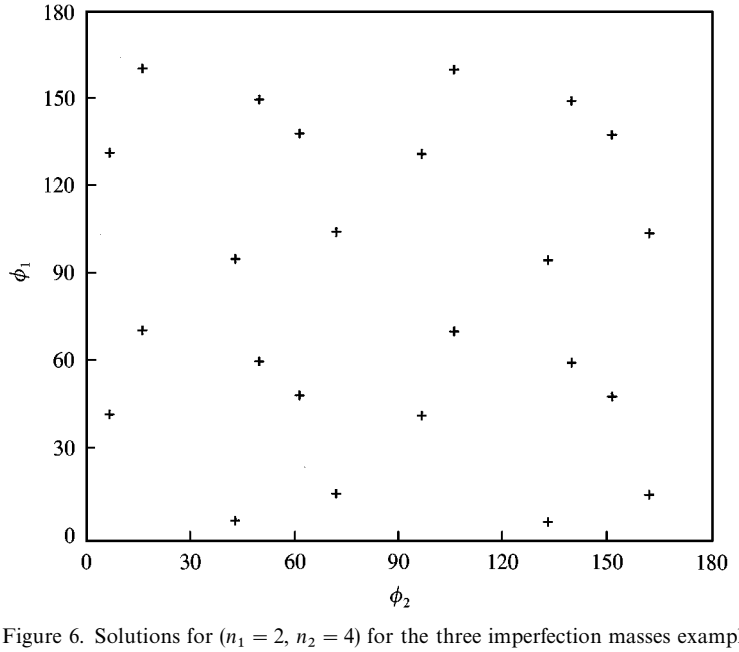

Figure 6. Solutions for ($n_1 = 2$, $n_2 = 4$) for the three imperfection masses example.

mass and a single spring have been attached. Next, a ring with a more complex form of imperfection is considered.

(3) *Three imperfection masses.* Consider the attachment of three imperfection masses (0·1, 0·2 and 0·3 kg) at pre-defined angular locations (0, 20 and 70°, respectively) on the initially perfect ring. The cases considered here correspond to trimming all possible pairs of modes when the number of nodal diameters $n = 2, 3, 4, 5$. Figures 5–10 show the complete set of

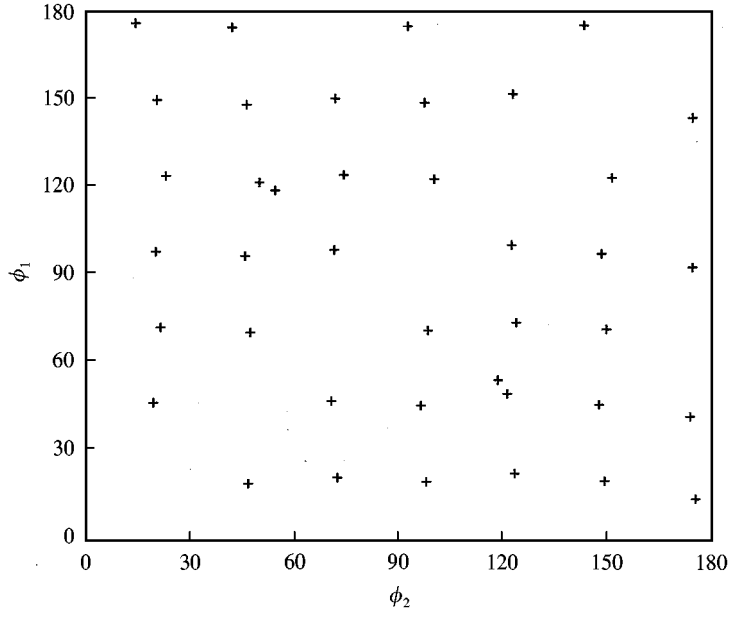

Figure 7. Solutions for ($n_1 = 2$, $n_2 = 5$) for the three imperfection masses example.

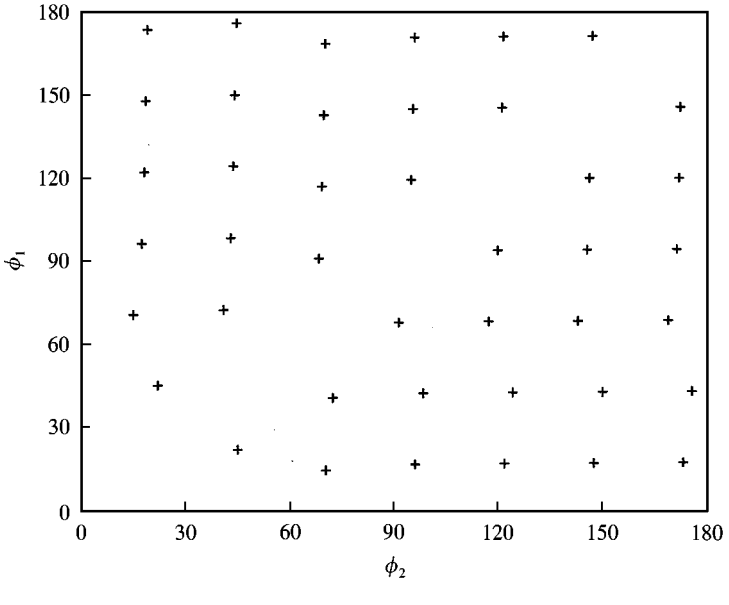

Figure 8. Solutions for ($n_1 = 3$, $n_2 = 4$) for the three imperfection masses example.

angular solutions to equations (33) and (34), as calculated using the described graphical method, for the specified pairs of modes. As with the previous two examples, the effect that different pairs of trimming masses have on the $n = 2, 3, 4, 5$ pairs of modes is recorded in Table 3 for the case when $n_1 = 2$ and $n_2 = 3$.

It can be seen from Table 3 that, as expected, the $n = 2$ and 3 modes are trimmed, while the frequency splits for the $n = 4$ and 5 modes have not been eliminated. The effect that the

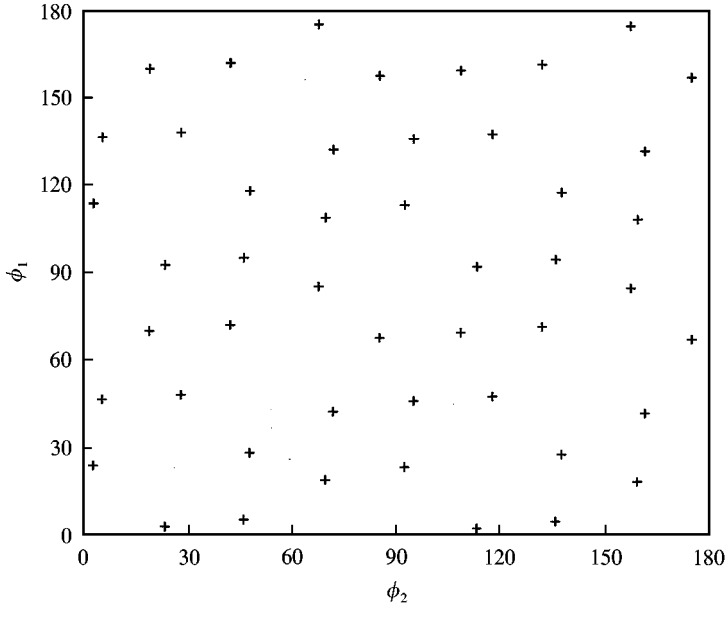

Figure 9. Solutions for ($n_1 = 3$, $n_2 = 5$) for the three imperfection masses example.

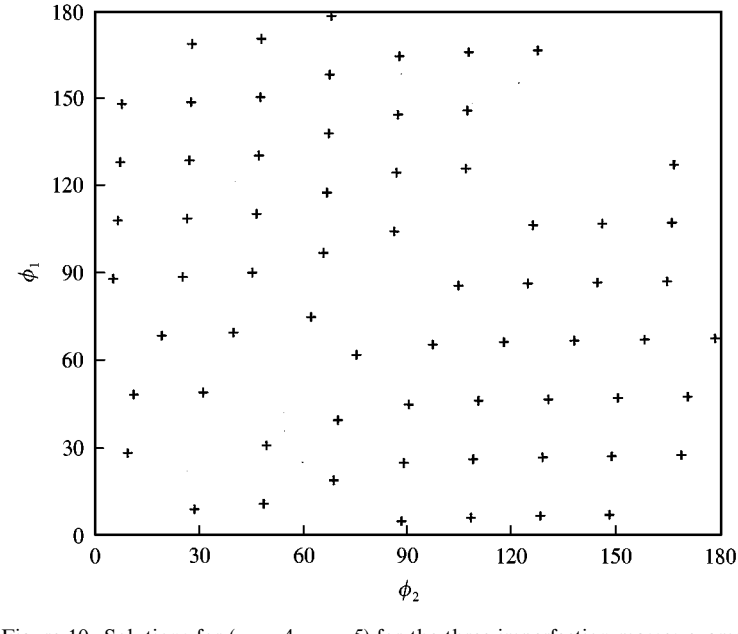

Figure 10. Solutions for ($n_1 = 4$, $n_2 = 5$) for the three imperfection masses example.

trimming masses have on these latter modes is varied. Some of the frequency splits are increased, whilst others are reduced. A comparison of these results with similar results obtained for the cases when $n_1 = 2$, $n_2 = 4$ and $n_1 = 3$, $n_2 = 4$ (see Figures 6 and 8) indicate that with careful calculations, the frequency splits of certain modes may be deliberately

TABLE 3

Trimming mass solutions for dual-mode trimming case (3)

Trimming masses				$n = 2$			$n = 3$			$n = 4$			$n = 5$		
ϕ_1 (deg)	m_1 (kg)	ϕ_2 (deg)	m_2 (kg)	ψ_n (deg)	ω_{n1} (Hz)	ω_{n2} (Hz)	ψ_n (deg)	ω_{n1} (Hz)	ω_{n2} (Hz)	ψ_n (deg)	ω_{n1} (Hz)	ω_{n2} (Hz)	ψ_n (deg)	ω_{n1} (Hz)	ω_{n2} (Hz)
—	—	—	—	− 6·95	35·056	35·656	11·82	97·832	102·423	23·16	188·02	195·89	− 4·14	305·71	314·97
3·95	− 0·523	144·31	− 0·398	Dg.	37·602		Dg.	106·355		27·11	190·69	220·36	4·09	348·53	313·78
6·86	− 0·298	107·92	0·248	Dg.	35·483		Dg.	100·362		23·74	184·87	201·01	− 5·36	301·53	321·88
12·90	− 0·199	71·00	− 0·262	Dg.	36·437		Dg.	103·059		28·54	196·00	199·25	− 7·77	314·11	325·33
37·63	0·406	172·18	0·195	Dg.	34·115		Dg.	96·493		32·84	179·93	190·56	− 2·17	288·99	310·60
40·65	0·335	134·82	− 0·133	Dg.	34·934		Dg.	98·809		28·03	186·30	192·78	2·55	298·52	314·92
44·02	0·327	97·15	0·159	Dg.	34·346		Dg.	97·145		29·24	186·92	185·62	0·01	298·01	304·56
75·07	− 0·327	155·81	0·185	Dg.	35·690		Dg.	100·947		17·87	188·46	199·08	4·49	317·66	308·58
77·86	− 0·480	119·16	− 0·293	Dg.	37·216		Dg.	105·263		12·66	193·83	210·91	− 8·66	309·93	345·82
111·48	0·522	150·52	0·478	Dg.	33·348		Dg.	94·321		19·92	170·80	192·91	3·43	278·58	308·68

Dg. indicates a degenerate pair of modes.

reduced. For example, it is found that the addition of a mass of 0·131 kg at 96·95° and a mass of 0·305 kg at 43·24° simultaneously trims the $n = 2$ and 4 modes, while the addition of a mass of 0·133 kg at 98·66° and a mass of 0·335 kg at 43·05° simultaneously trims the $n = 3$ and 4 modes. Hence, the addition of a mass of 0·159 kg at 97·15° and a mass of 0·327 kg at 44·02° significantly reduces the frequency split of the $n = 4$ mode.

This has more significance in a theoretical investigation than in a physical trimming procedure. The sensitivity of physical equipment limits the accuracy of the angular positions. Also, the trimming masses have been described as point masses but in reality they will have a finite width that may overlap all three combinations of angles. Thus, the above comparison considers the ideal situation.

Nonetheless, the frequency split in the $n = 4$ mode still is larger than is usually desirable so it seems infeasible that two trimming masses can be used to trim more than two modes simultaneously.

In summary, it has been demonstrated, for the three cases considered, that it is possible to simultaneously eliminate the frequency splits of two pairs of modes by the addition of two masses to an initially imperfect ring. In addition, it has been shown that in general it is not possible to deliberately trim more than two pairs of modes with only two trimming masses.

5. MULTI-MODE FREQUENCY TRIMMING

The basis of the method for trimming three or more pairs of modes simultaneously was described in section 2. To calculate the angular locations of the trimming masses it is necessary to find solutions to equation (20). Given that the matrix appearing on the left-hand side of this equation involves the inverse of matrix **B**, it is inevitable that the resulting simultaneous equations will be highly non-linear in terms of trimming mass location and that simple analytical solutions are not possible. Indeed, the authors consider the relationships arising from the tri-mode trimming case too complex for analytical manipulation. For this reason, it is necessary to resort to numerical techniques. One numerical procedure that is well-suited to this particular problem is to square each of the simultaneous equations appearing in equation (20), take the sum of these squares, and then find the angular positions ϕ_i $(i = 1, 2, \ldots, N)$ that ensure the single resultant equation is zero. That is, calculate the solutions to:

$$\sum_{i=1}^{N} \left(\sum_{j=1}^{N} f_{ij} \lambda_{n_j} \right)^2 = 0, \tag{46}$$

where f_{ij} is the ijth element of the matrix $\mathbf{AB}^{-1}$, which can be calculated easily. Following the numerical solution of this equation, the trimming masses can be calculated using equation (19). Thus, it should be possible to simultaneously trim the frequency splits of N $n\theta$ modes using N trimming masses. This method will be tested in the following numerical example for $N = 3$.

Consider the attachment of three imperfection masses (0·1, 0·2 and 0·3 kg) at pre-defined angular locations (0, 20 and 70°, respectively) on the initially perfect ring in a similar way to those considered in case (3) for dual-mode trimming. It has been hypothesized that three vibrational modes can be simultaneously trimmed by the addition of three trimming masses. The example that is to be considered is the trimming of the first three vibrational modes ($n_1 = 2, n_2 = 3, n_3 = 4$) with the effect of the three trimming masses on the next mode ($n_4 = 5$) also being illustrated.

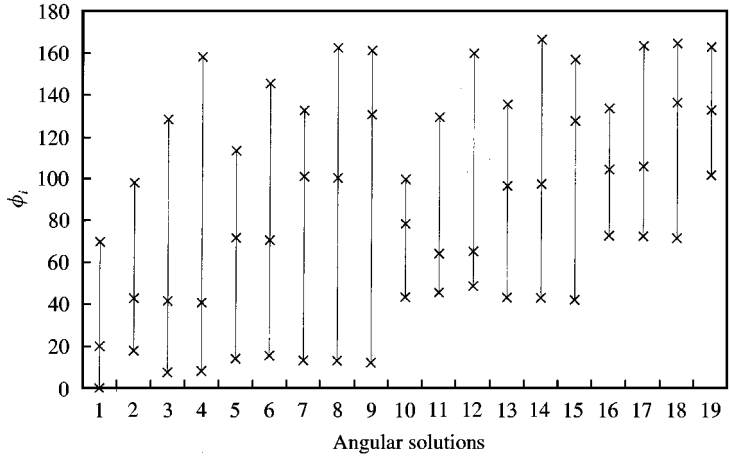

Figure 11. Solutions for ($n_1 = 2$, $n_2 = 3$, $n_3 = 4$) for the three trimming masses example.

Using an iterative search process based on a grid search method [14], a set of solutions to equation (46) were calculated when $N = 3$. The complete set of angular solutions found is shown in Figure 11. Nineteen unique triplets of angular positions were found and each triplet is shown by a vertical line with the three angular solutions in each triplet represented by a cross. It can be observed from Figure 11 that the angular solutions tend to lie within certain regions. This suggests that there may be a grid of intersecting planes akin to the grid of intersecting lines that represents the angular solutions for two trimming masses. However, the equations that describe these planes are not obvious from either the numerical example or from the analysis of equations (20) and (21) for $N = 3$. As in previous examples, some of the solutions have been highlighted in a table but for clarity, not all of the solutions have been included. The solutions are recorded in Table 4.

As expected, the trivial solution of removing the original imperfection masses from the positions at which they had been attached has been obtained. This solution eliminates the frequency splits from all the modes of the ring and this has been shown for the first four modes. This is the only case in which the $n_4 = 5$ mode is trimmed. The other three modes have been trimmed to degenerate pairs of modes as shown for each triplet of trimming masses. As was the situation for two trimming masses, the trimming masses are required to be either added to or removed from the ring. This means that both methods of trimming can be successfully used.

A comparison of solutions for tri-mode and dual-mode trimming clarifies, for one pair of angular solutions, the coincidental trimming of the $n_3 = 4$ mode when the $n_1 = 2$ and $n_2 = 3$ modes were being trimmed in the dual-mode trimming process. As shown in Table 4, the addition of trimming masses at 44·02 and 97·15° significantly reduced the frequency split of the $n = 4$ mode. Now, considering Table 4, it can be seen that there is a comparable pair of trimming masses at similar angular positions with the addition of a third significantly smaller mass on the ring.

Hence, it has been shown that it is possible to calculate the three trimming masses that are required to simultaneously eliminate the frequency splits from three modes using a numerical method. The same numerical method can then be used to calculate N trimming masses to simultaneously eliminate N frequency splits.

TABLE 4

Trimming mass solutions for the tri-mode frequency trimming case

Trimming masses						$n = 2$			$n = 3$			$n = 4$			$n = 5$		
ϕ_1 (deg)	m_1 (kg)	ϕ_2 (deg)	m_2 (kg)	ϕ_3 (deg)	m_3 (kg)	ψ_n (deg)	ω_{n1} (Hz)	ω_{n2} (Hz)	ψ_n (deg)	ω_{n1} (Hz)	ω_{n2} (Hz)	ψ_n (deg)	ω_{n1} (Hz)	ω_{n2} (Hz)	ψ_n (deg)	ω_{n1} (Hz)	ω_{n2} (Hz)
—	—	—	—	—	—	− 6·95	35·056	35·656	11·82	97·832	102·423	23·16	188·02	195·89	− 4·14	305·71	314·97
0	− 0·1	20	− 0·2	70	− 0·3	Dg.	36·779		Dg.	104·026		Dg.	199·46		Dg.	322·57	322·57
7·54	0·128	41·73	0·438	128·35	− 0·145	Dg.	34·477		Dg.	97·514		Dg.	186·97		3·25	291·31	314·81
12·26	− 0·759	130·75	− 0·577	161·50	− 0·874	Dg.	41·584		Dg.	117·617		Dg.	225·52		− 1·39	319·10	437·89
43·42	0·327	96·97	0·131	135·70	− 0·023	Dg.	34·448		Dg.	97·434		Dg.	186·82		1·06	298·25	306·16
72·93	− 0·475	106·30	− 0·206	163·92	0·174	Dg.	36·550		Dg.	103·379		Dg.	198·22		2·10	334·92	307·91
102·18	0·759	133·10	0·951	163·28	0·650	Dg.	31·084		Dg.	87·919		Dg.	168·57		7·93	298·98	252·20

Dg. indicates a degenerate pair of modes.

TABLE 5

Rayleigh–Ritz analysis of the effect of the addition of imperfection masses to a perfect ring

Imperfection masses (magnitude and angular position)						Natural frequencies and orientations for one generalized coordinate		Rayleigh–Ritz solutions for three generalized co-ordinates				
								Natural frequencies	Ratio of displacements	Orientations		
m_1 (kg)	ϕ_1 (deg)	m_2 (kg)	ϕ_2 (deg)	m_3 (kg)	ϕ_3 (deg)	ω_n (Hz)	ψ_n (deg)	ω_n (Hz)	$U_1:U_2:U_3$	ψ_1 (deg)	ψ_2 (deg)	ψ_3 (deg)
0·01233	0	0·02466	20	0·03699	70	36·5585	− 6·95	36·5592	0·0127:1:0·0013	32·50	− 6·91	10·44
						36·6350	38·05	36·6363	0·0133:1:0·0004	− 54·02	38·09	− 23·39
						103·1995	11·82	103·2115	0·0138:0·0210:1	36·46	− 4·22	11·84
						103·8257	− 18·18	103·8272	0·0072:0·0066:1	− 44·20	− 44·21	− 18·16
0·1	0	0·2	20	0·3	70	35·096	− 6.95	35·137	0·0967:1:0·0096	33·01	− 6·67	10·32
						35·656	38·05	35·728	0·1013:1:0·0030	− 53·59	38·33	− 23·25
						97·832	11·82	98·435	0·0917:0·1541:1	36·49	− 4·22	12·00
						102·423	− 18.18	102·512	0·0504:0·0487:1	− 43·72	− 43·65	− 18·01

6. CONCLUSION

A method of calculating the trimming masses needed to simultaneously trim a number of pairs of modes of a ring has been described. This has been achieved by extending the concept of "equivalent imperfection mass" proposed by Fox [7] to multiple pairs of modes. It is found for the case of dual-mode trimming that a graphical method can be used to aid the calculations, and that two trimming masses can be used to trim two pairs of modes. The method is validated through theoretical calculations for rings with imperfections arising from the attachment of discrete masses and springs. In order to trim three or more pairs of modes a numerical method is proposed. The validity of this method has been verified for tri-mode frequency trimming of a specific numerical example, and it can be inferred from this that the numerical method can be used to trim more than three pairs of modes.

ACKNOWLEDGMENT

The authors gratefully acknowledge the support for this work provided by BAE SYSTEMS and EPSRC under the Industrial CASE scheme.

REFERENCES

1. I. HOPKIN 1997 *Proceedings of DGON Symposium on Gyro Technology*, *Stuttgart*, Chapter 1. Performance and design of a silicon micro-machined gyro.
2. S. A. TOBIAS 1951 *Engineering* **172**, 409–410. A theory of imperfection for elastic bodies of revolution.
3. R. PERRIN 1971 *Acustica* **25**, 69–72. Selection rules for the splitting of the degenerate pairs of natural frequencies of thin circular rings.
4. T. CHARNLEY and R. PERRIN 1973 *Acustica* **28**, 139–146. Perturbation studies with a thin circular ring.
5. P. A. A. LAURA, C. P. FILIPICH, R. E. ROSSI and J. A. REYES 1988 *Applied Acoustics* **25**, 225–234. Vibrations of rings of variable cross section.
6. R. F. TONIN and D. A. BIES 1979 *Journal of Sound and Vibration* **62**, 165–180. Free vibration of a circular cylinder with variable thickness.
7. C. H. J. FOX 1990 *Journal of Sound and Vibration* **142**, 227–243. A simple theory for the analysis and correction of frequency splitting in slightly imperfect rings.
8. C. H. J. FOX 1997 *Proceedings of* XV *International Modal Analysis Conference*, *Tokyo*, 566–572. Mode trimming in nominally axi-symmetric structures.
9. R. S. HWANG, C. H. J. FOX and S. MCWILLIAM 1999 *Journal of Sound and Vibration* **220**, 497–516. The in-plane vibration of thin rings with in-plane profile variations. Part I: general background and theoretical formulation.
10. C. H. J. FOX, R. S. HWANG and S. MCWILLIAM 1999 *Journal of Sound and Vibration* **220**, 517–539. The in-plane vibration of thin rings with in-plane profile variations. Part II: application to nominally circular rings.
11. R. S. HWANG, C. H. J. FOX and S. MCWILLIAM 1999 *Journal of Sound and Vibration* **228**, 683–699. Free vibrations of elliptical rings with circumferentially variable thickness.
12. R. ELEY, C. H. J. FOX and S. MCWILLIAM 1999 *Journal of Sound and Vibration* **228**, 11–35. Anisotropy effects on the vibration of circular rings made from crystalline silicon.
13. A. K. ROURKE 2000 *Internal Report of the School of Mechanical*, *Materials*, *Manufacturing Engineering and Management*, *University of Nottingham*. The simultaneous trimming of two frequency splits for an imperfect ring.
14. S. S. RAO *Engineering Optimisation*: *Theory and Practice*. New York: John-Wiley & Son: third edition.
15. G. B. WARBURTON 1965 *Institution of Mechanical Engineers Journal of Mechanical Engineering Science* **7**, 399–407. Vibration of thin cylindrical shells.

APPENDIX A: RAYLEIGH–RITZ ANALYSIS OF THE EFFECT OF IMPERFECTION MASSES ON THE NATURAL FREQUENCIES AND MODE SHAPES OF A PERFECT RING

It is possible to test the assumption that the mode shapes of a ring will be unaffected by small imperfection masses by performing a Rayleigh–Ritz analysis on the ring. This analysis has been performed using the first three generalized co-ordinates of the ring and these results are compared with the mode shapes assumed in equations (1)–(4) and the natural frequencies and orientations, which are given by equations (7), (8) and (9). The analysis has been simplified by fixing the amplitude ratio, α_n, of the nth co-ordinate as n, where $\alpha_n = W_n/U_n$. This is a valid substitution provided that it is the in-plane flexural modes of the ring that are being considered.

The results of this analysis are recorded in Table 5 for the first two elastic modes of vibration, which are modified forms of the $n = 2$ and 3 modes. The perfect ring that has been used is the same ring as that considered for the other numerical examples. The mass of this ring is 7·3984 kg and the first set of imperfection masses have been chosen to total 1% of this mass. Initially, it is assumed that the mode shapes of the first two elastic modes of vibration can be approximated as the displacement of one generalized co-ordinate, $n\theta$, as indicated by equations (1)–(4). Thus, the frequency splits and orientations of these two modes can be calculated from equations (7) to (9) and these are the data recorded in the central column of Table 5. A Rayleigh–Ritz analysis has then been performed using the first three generalized co-ordinates ($n = 1$, 2, 3). The natural frequencies of the first two elastic modes and the relative displacements and orientations of the generalized co-ordinates have been calculated, and recorded in the final set of columns of Table 5, for each natural frequency.

On comparing the natural frequencies that have been found by the single generalized co-ordinate and the three generalized co-ordinates methods, it can be seen that the difference between the two methods for the natural frequencies of the first elastic mode is less than 0·01%, which is the largest desirable frequency split in any mode, as was mentioned earlier. The largest difference between the two methods for the natural frequencies of the second elastic mode is 0·01%. Thus, the differences between the two methods are within the required tolerances for a combined imperfection mass of 1% of the total mass of the ring. Also, considering the ratio of the displacements of the three generalized co-ordinates, it can be seen that for the first elastic mode it is the displacement of the second generalized co-ordinate that is dominant and the orientation of the second generalized co-ordinate is close to the orientation of the single co-ordinate solution. A similar result can be observed for the second elastic mode.

For emphasis, the numerical examples recorded in Tables 1–4 have used larger imperfection masses than is ideal. However, the second set of frequency splits recorded in Table 5 shows that even for imperfection masses that are almost 10% of the total mass of the ring, the variation of the natural frequencies is less than 1%. In addition, the displacement of the nth generalized co-ordinate is still the dominant term for the displacement of the nth mode.

Thus, it can be seen that it is reasonable to assume that the mode shapes of an imperfect ring are identical to those of the perfect ring from which it was formed.

APPENDIX B: DERIVATION OF VALUES FOR THE NATURAL FREQUENCY, ω_{0n}, AND THE AMPLITUDE RATIO, α_n, OF A PERFECT RING

The natural frequency of the perfect ring can be found by considering the kinetic energy, $\omega_{0n}^2 T$, and strain energy, S, of the ring. These are given in Appendix 2 of reference [15],

having assumed Flügge's strain–displacement relations, after integrating through the thickness of the shell. To remain consistent with the orientations of the radial and tangential motion of the ring as given in reference [7] it has been necessary to modify the equations given in reference [15] by replacing v with u, u with $-v$ and x with $-y$. Also, the mean radius of the ring has been changed from a to R. Another modification to the equations given in reference [15] is that the terms that form perfect squares have been collected to produce a more manageable equation.

$$\omega_{0n}^2 T_{0n} = \frac{Rh\rho}{2} \int_0^{2\pi} \int_0^L \left[\left(\frac{\partial u}{\partial t}\right)^2 + \left(\frac{\partial v}{\partial t}\right)^2 + \left(\frac{\partial w}{\partial t}\right)^2 \right] \mathrm{d}y\, \mathrm{d}\phi, \tag{B1}$$

$$S_{0n} = \frac{ERh}{2(1-\nu^2)} \int_0^{2\pi} \int_0^L \left[\left(\frac{\partial v}{\partial y}\right)^2 + \frac{1}{R^2}\left(\frac{\partial u}{\partial \phi} - w\right)^2 + \frac{2\nu}{R}\frac{\partial v}{\partial y}\left(\frac{\partial u}{\partial \phi} - w\right) + \frac{(1-\nu)}{2}\left(\frac{\partial u}{\partial y} + \frac{1}{R}\frac{\partial v}{\partial \phi}\right)^2 \right.$$
$$\left. + \beta \left\{ R^2 \left(\frac{\partial^2 w}{\partial y^2}\right)^2 + \frac{1}{R^2}\left(\frac{\partial^2 w}{\partial \phi^2} + w\right)^2 + 2\nu \frac{\partial^2 w}{\partial y^2}\left(\frac{\partial^2 w}{\partial \phi^2} + \frac{\partial u}{\partial \phi}\right) + 2R \frac{\partial v}{\partial y}\frac{\partial^2 w}{\partial y^2} \right.\right.$$
$$\left.\left. + (1-\nu)\left\{ 2\left(\frac{\partial^2 w}{\partial y \partial \phi}\right)^2 + \frac{1}{2R^2}\left(\frac{\partial v}{\partial \phi}\right)^2 - \frac{1}{R}\frac{\partial v}{\partial \phi}\frac{\partial^2 w}{\partial y \partial \phi} \right.\right.\right.$$
$$\left.\left.\left. + \frac{3}{2}\left(\frac{\partial u}{\partial y}\right)^2 + 3\frac{\partial u}{\partial y}\frac{\partial^2 w}{\partial y \partial \phi} \right\} \right\} \right] \mathrm{d}y\, \mathrm{d}\phi. \tag{B2}$$

It has been assumed that the axial length of the cylinder is short enough so that there is no variation in the dependence of the vibrational motion on the axial position, y, of an element of the ring. Therefore, terms involving differentiation with respect to y have been neglected from the strain energy equation.

$$S_{0n} = \frac{ERh}{2(1-\nu^2)} \int_0^{2\pi} \int_0^L \left[\frac{1}{R^2}\left(\frac{\partial u}{\partial \phi} - w\right)^2 + \frac{(1-\nu)}{2R^2}\left(\frac{\partial v}{\partial \phi}\right)^2 + \beta \left\{ \frac{1}{R^2}\left(\frac{\partial^2 w}{\partial \phi^2} + w\right)^2 \right.\right.$$
$$\left.\left. + \frac{(1-\nu)}{2R^2}\left(\frac{\partial v}{\partial \phi}\right)^2 \right\} \right] \mathrm{d}y\, \mathrm{d}\phi. \tag{B3}$$

Equation (B3) can also be expressed as

$$S_{0n} = \frac{EhL}{2R(1-\nu^2)} \int_0^{2\pi} \left[\left(\frac{\partial u}{\partial \phi} - w\right)^2 + (1-\nu)(1+\beta)\left(\frac{\partial v}{\partial \phi}\right)^2 + \beta\left(\frac{\partial^2 w}{\partial \phi^2} + w\right)^2 \right] \mathrm{d}\phi. \tag{B4}$$

For in-plane vibrations, it is possible to neglect the axial motion, which is represented by $v(\phi, t)$. The kinetic and strain energies can then be found by substitution of the correct forms of the radial and tangential displacements, which are:

$$w(\phi, t) = W \cos n\phi \exp(\mathrm{i}\omega_{0n} t), \qquad u(\phi, t) = U \sin n\phi \exp(\mathrm{i}\omega_{0n} t). \tag{B5, B6}$$

By substituting equations (B5) and (B6) into equations (B4) and (B1), and setting the amplitude ratio $\alpha_n = W/U$, it can be seen that

$$S_{0n} = \frac{U^2 EhL\pi}{2R(1-\nu^2)}\left((n-\alpha_n)^2 + \beta\alpha_n^2(1-n^2)^2\right), \tag{B7}$$

$$\omega_{0n}^2 T_{0n} = \omega_{0n}^2\, U^2 RhL\rho\pi(1+\alpha_n^2)/2. \tag{B8}$$

The natural frequency, ω_{0n}, which can be found from the ratio of the strain and kinetic energies is therefore,

$$\omega_{0n}^2 = \frac{S_{0n}}{T_{0n}} = \frac{E\left((n-\alpha_n)^2 + \beta\alpha_n^2(1-n^2)^2\right)}{R^2\rho(1-\nu^2)(1+\alpha_n^2)}. \tag{B9}$$

Finally, the amplitude ratio, α_n, can be found from the Rayleigh–Ritz method by setting $\partial\omega_{0n}^2/\partial\alpha_n = 0$.

$$\frac{\partial\omega_{0n}^2}{\partial\alpha_n} = \frac{2En}{R^2\rho(1-\nu^2)(1+\alpha_n^2)^2}\left\{\alpha_n^2 + \alpha_n\frac{(1-n^2)(1+\beta(1-n^2))}{n} - 1\right\}. \tag{B10}$$

It can be easily seen from equation (B10) that

$$\alpha_n = \frac{(n^2-1)(1+\beta(1-n^2))}{2n} \pm \sqrt{\frac{(1-n^2)^2(1+\beta(1-n^2))^2}{4n^2} - 1}\,. \tag{B11}$$

From equation (B11), two amplitude ratios arise, one corresponding to the flexural modes and the other corresponding to the extensional modes.

For many practical rings, the constant β is small and terms containing β can be neglected in equation (B11). In those cases, the amplitude ratio of the flexural mode can be shown to be equal to n and that of the extensional mode can be shown to be equal to $-1/n$. This will simplify the expression for the natural frequency of a perfect ring.

This paper deals primarily with the flexural modes of the ring and so equation (B9) can be simplified for these modes by a substitution of $\alpha_n = n$. Hence,

$$\omega_{0n}^2 = \frac{E\beta(1-n^2)^2 n^2}{R^2\rho(1-\nu^2)(1+n^2)}. \tag{B12}$$

APPENDIX C: DERIVATION OF EQUATION (29)

By substituting the matrix **A** shown in equation (26) into equation (21) it can be seen that

$$\begin{vmatrix} \sin 2n_1(\phi_1 - \psi_{n_1}) & \sin 2n_1(\phi_2 - \psi_{n_1}) \\ \sin 2n_2(\phi_1 - \psi_{n_2}) & \sin 2n(\phi_2 - \psi_{n_2}) \end{vmatrix} = 0. \tag{C1}$$

Manipulation of this determinant creates the following two equations from which the relationship between ϕ_1 and ϕ_2 can be found. The manipulations made use of the rule that the size of the determinant will remain unchanged if one line is added to or deducted from another line.

$$\begin{vmatrix} \sin 2n_1(\phi_1 - \psi_{n_1}) + \sin 2n_2(\phi_1 - \psi_{n_2}) & \sin 2n_1(\phi_2 - \psi_{n_1}) + \sin 2n_2(\phi_2 - \psi_{n_2}) \\ \sin 2n_2(\phi_1 - \psi_{n_2}) & \sin 2n_2(\phi_2 - \psi_{n_2}) \end{vmatrix} = 0, \tag{C2}$$

$$\begin{vmatrix} \sin 2n_1(\phi_1 - \psi_{n_1}) - \sin 2n_2(\phi_1 - \psi_{n_2}) & \sin 2n_1(\phi_2 - \psi_{n_1}) - \sin 2n_2(\phi_2 - \psi_{n_2}) \\ \sin 2n_2(\phi_1 - \psi_{n_2}) & \sin 2n_2(\phi_2 - \psi_{n_2}) \end{vmatrix} = 0. \quad \text{(C3)}$$

Expanding these two determinants and rearranging produces the following equations:

$$\frac{\sin 2n_2(\phi_1 - \psi_{n_2})}{\sin 2n_2(\phi_2 - \psi_{n_2})} = \frac{\sin 2n_1(\phi_1 - \psi_{n_1}) + \sin 2n_2(\phi_1 - \psi_{n_2})}{\sin 2n_1(\phi_2 - \psi_{n_1}) + \sin 2n_2(\phi_2 - \psi_{n_2})}, \quad \text{(C4)}$$

$$\frac{\sin 2n_2(\phi_1 - \psi_{n_2})}{\sin 2n_2(\phi_2 - \psi_{n_2})} = \frac{\sin 2n_1(\phi_1 - \psi_{n_1}) - \sin 2n_2(\phi_1 - \psi_{n_2})}{\sin 2n_1(\phi_2 - \psi_{n_1}) - \sin 2n_2(\phi_2 - \psi_{n_2})}. \quad \text{(C5)}$$

Equations (C4) and (C5) can be rearranged, using standard trigonometric identities, into the following forms:

$$\frac{\sin 2n_2(\phi_1 - \psi_{n_2})}{\sin 2n_2(\phi_2 - \psi_{n_2})} = \frac{\sin((n_1 + n_2)\phi_1 - n_1\psi_{n_1} - n_2\psi_{n_2}) \cos((n_1 - n_2)\phi_1 - n_1\psi_{n_1} + n_2\psi_{n_2})}{\sin((n_1 + n_2)\phi_2 - n_1\psi_{n_1} - n_2\psi_{n_2}) \cos((n_1 - n_2)\phi_2 - n_1\psi_{n_1} + n_2\psi_{n_2})}, \quad \text{(C6)}$$

$$\frac{\sin 2n_2(\phi_1 - \psi_{n_2})}{\sin 2n_2(\phi_2 - \psi_{n_2})} = \frac{\cos((n_1 + n_2)\phi_1 - n_1\psi_{n_1} - n_2\psi_{n_2}) \sin((n_1 - n_2)\phi_1 - n_1\psi_{n_1} + n_2\psi_{n_2})}{\cos((n_1 + n_2)\phi_2 - n_1\psi_{n_1} - n_2\psi_{n_2}) \sin((n_1 - n_2)\phi_2 - n_1\psi_{n_1} + n_2\psi_{n_2})}. \quad \text{(C7)}$$

Equating the right-hand sides of equations (C6) and (C7) produces the following equation:

$$\frac{\sin((n_1 + n_2)\phi_1 - n_1\psi_{n_1} - n_2\psi_{n_2}) \cos((n_1 - n_2)\phi_1 - n_1\psi_{n_1} + n_2\psi_{n_2})}{\sin((n_1 + n_2)\phi_2 - n_1\psi_{n_1} - n_2\psi_{n_2}) \cos((n_1 - n_2)\phi_2 - n_1\psi_{n_1} + n_2\psi_{n_2})}$$
$$= \frac{\cos((n_1 + n_2)\phi_1 - n_1\psi_{n_1} - n_2\psi_{n_2}) \sin((n_1 - n_2)\phi_1 - n_1\psi_{n_1} + n_2\psi_{n_2})}{\cos((n_1 + n_2)\phi_2 - n_1\psi_{n_1} - n_2\psi_{n_2}) \sin((n_1 - n_2)\phi_2 - n_1\psi_{n_1} + n_2\psi_{n_2})}, \quad \text{(C8)}$$

which also can be expressed as

$$\tan((n_1 + n_2)\phi_1 - n_1\psi_{n_1} - n_2\psi_{n_2}) \tan((n_1 - n_2)\phi_2 - n_1\psi_{n_1} + n_2\psi_{n_2})$$
$$= \tan((n_1 + n_2)\phi_2 - n_1\psi_{n_1} - n_2\psi_{n_2}) \tan((n_1 - n_2)\phi_1 - n_1\psi_{n_1} + n_2\psi_{n_2}). \quad \text{(C9)}$$

APPENDIX D: DERIVATION OF EQUATIONS (30) AND (31)

Substitution of equations (26), (27) and (28) into equation (20) produces the following pair of simultaneous equations:

$$M \frac{\begin{pmatrix} \lambda_{n_1}(\sin 2n_1(\phi_1 - \psi_{n_1}) \cos 2n_2(\phi_2 - \psi_{n_2}) - \sin 2n_1(\phi_2 - \psi_{n_1}) \cos 2n_2(\phi_1 - \psi_{n_2})) \\ + \lambda_{n_2}(\sin 2n_1(\phi_2 - \psi_{n_1}) \cos 2n_1(\phi_1 - \psi_{n_1}) - \sin 2n_1(\phi_1 - \psi_{n_1}) \cos 2n_1(\phi_2 - \psi_{n_1})) \end{pmatrix}}{\cos 2n_1(\phi_1 - \psi_{n_1}) \cos 2n_2(\phi_2 - \psi_{n_2}) - \cos 2n_1(\phi_2 - \psi_{n_1}) \cos 2n_2(\phi_1 - \psi_{n_2})} = 0, \quad \text{(D1)}$$

$$M\frac{\begin{pmatrix}\lambda_{n_1}(\sin 2n_2(\phi_1-\psi_{n_2})\cos 2n_2(\phi_2-\psi_{n_2})-\sin 2n_2(\phi_2-\psi_{n_2})\cos 2n_2(\phi_1-\psi_{n_2}))\\+\lambda_{n_2}(\sin 2n_2(\phi_2-\psi_{n_2})\cos 2n_1(\phi_1-\psi_{n_1})-\sin 2n_2(\phi_1-\psi_{n_2})\cos 2n_1(\phi_2-\psi_{n_1}))\end{pmatrix}}{\cos 2n_1(\phi_1-\psi_{n_1})\cos 2n_2(\phi_2-\psi_{n_2})-\cos 2n_1(\phi_2-\psi_{n_1})\cos 2n_2(\phi_1-\psi_{n_2})}=0. \tag{D2}$$

Either of equations (D1) and (D2) may be used to produce the same overall solutions. The choice of equation must be consistent with the choice made in Appendix C as a similar relationship to that shown by equations (C6) and (C7) needs to be found. Thus, equation (D2) is manipulated into the form:

$$\frac{\sin 2n_2(\phi_1-\psi_{n_2})}{\sin 2n_2(\phi_2-\psi_{n_2})}=\frac{\lambda_{n_2}\cos 2n_1(\phi_1-\psi_{n_1})-\lambda_{n_1}\cos 2n_2(\phi_1-\psi_{n_2})}{\lambda_{n_2}\cos 2n_1(\phi_2-\psi_{n_1})-\lambda_{n_1}\cos 2n_2(\phi_2-\psi_{n_2})} \tag{D3}$$

By re-expressing each of the cosine terms, equation (D3) can be expanded into a form that is more comparable with equations (C6) and (C7). Consider the expansion of

$$\cos 2n_1(\phi_1-\psi_{n_1})=\frac{\cos 2n_1(\phi_1-\psi_{n_1})+\cos 2n_2(\phi_1-\psi_{n_2})}{2}+\frac{\cos 2n_1(\phi_1-\psi_{n_1})-\cos 2n_2(\phi_1-\psi_{n_2})}{2}. \tag{D4}$$

This can be rearranged, using standard trigonometric identities, to show that

$$\begin{aligned}\cos 2n_1(\phi_1-\psi_{n_1})=&\cos((n_1+n_2)\phi_1-n_1\psi_{n_1}-n_2\psi_{n_2})\cos((n_1-n_2)\phi_1-n_1\psi_{n_1}+n_2\psi_{n_2})\\&-\sin((n_1+n_2)\phi_1-n_1\psi_{n_1}-n_2\psi_{n_2})\sin((n_1-n_2)\phi_1-n_1\psi_{n_1}+n_2\psi_{n_2}).\end{aligned} \tag{D5}$$

Performing the same manipulations on each of the cosine terms in equation (D3) will re-express equation (D3) as

$$\begin{aligned}\frac{\sin 2n_2(\phi_1-\psi_{n_2})}{\sin 2n_2(\phi_2-\psi_{n_2})}=&\\&\frac{\begin{array}{l}(\lambda_{n_2}-\lambda_{n_1})\cos((n_1+n_2)\phi_1-n_1\psi_{n_1}-n_2\psi_{n_2})\cos((n_2-n_1)\phi_1-n_2\psi_{n_2}+n_1\psi_{n_1})\\+(\lambda_{n_2}+\lambda_{n_1})\sin((n_1+n_2)\phi_1-n_1\psi_{n_1}-n_2\psi_{n_2})\sin((n_2-n_1)\phi_1-n_2\psi_{n_2}+n_1\psi_{n_1})\end{array}}{\begin{array}{l}(\lambda_{n_2}-\lambda_{n_1})\cos((n_1+n_2)\phi_2-n_1\psi_{n_1}-n_2\psi_{n_2})\cos((n_2-n_1)\phi_2-n_2\psi_{n_2}+n_1\psi_{n_1})\\+(\lambda_{n_2}+\lambda_{n_1})\sin((n_1+n_2)\phi_2-n_1\psi_{n_1}-n_2\psi_{n_2})\sin((n_2-n_1)\phi_2-n_2\psi_{n_2}+n_1\psi_{n_1})\end{array}}\end{aligned} \tag{D6}$$

Equations (30) and (31) can now be found by comparison of equation (D6) with equations (C6) and (C7) respectively. Equating the right-hand sides of equations (C6) and (D6) shows that

$$\begin{aligned}&(\lambda_{n_2}-\lambda_{n_1})\cot((n_1+n_2)\phi_1-n_1\psi_{n_1}-n_2\psi_{n_2})+(\lambda_{n_2}+\lambda_{n_1})\tan((n_2-n_1)\phi_1-n_2\psi_{n_2}+n_1\psi_{n_1})\\&\quad=(\lambda_{n_2}-\lambda_{n_1})\cot((n_1+n_2)\phi_2-n_1\psi_{n_1}-n_2\psi_{n_2})\\&\qquad+(\lambda_{n_2}+\lambda_{n_1})\tan((n_2-n_1)\phi_2-n_2\psi_{n_2}+n_1\psi_{n_1}).\end{aligned} \tag{D7}$$

This can also be written as

$$\frac{[(\lambda_{n_2}-\lambda_{n_1})-(\lambda_{n_1}+\lambda_{n_2})\tan((n_2-n_1)\phi_2-n_2\psi_{n_2}+n_1\psi_{n_1})\tan((n_1+n_2)\phi_1-n_1\psi_{n_1}-n_2\psi_{n_2})]}{\tan((n_1+n_2)\phi_1-n_1\psi_{n_1}-n_2\psi_{n_2})}$$

$$-\frac{\begin{array}{l}[(\lambda_{n_2}-\lambda_{n_1})-(\lambda_{n_1}+\lambda_{n_2})\tan((n_2-n_1)\phi_1-n_2\psi_{n_2}\\ +n_1\psi_{n_1})\tan((n_1+n_2)\phi_2-n_1\psi_{n_1}-n_2\psi_{n_2})]\end{array}}{\tan((n_1+n_2)\phi_2-n_1\psi_{n_1}-n_2\psi_{n_2})}=0. \tag{D8}$$

Substitution of equation (C9) simplifies equation (D8) into

$$\left(\tan((n_1+n_2)\phi_1-n_1\psi_{n_1}-n_2\psi_{n_2})\tan((n_2-n_1)\phi_2-n_2\psi_{n_2}+n_1\psi_{n_1})-\frac{\lambda_{n_2}-\lambda_{n_1}}{\lambda_{n_2}+\lambda_{n_1}}\right)$$
$$\times(\tan((n_1+n_2)\phi_1-n_1\psi_{n_1}-n_2\psi_{n_2})-\tan((n_1+n_2)\phi_2-n_1\psi_{n_1}-n_2\psi_{n_2}))=0. \tag{D9}$$

Likewise, equating equations (C7) and (D6) shows that

$$(\lambda_{n_2}-\lambda_{n_1})\cot((n_2-n_1)\phi_1-n_2\psi_{n_2}+n_1\psi_{n_1})+(\lambda_{n_2}+\lambda_{n_1})\tan((n_1+n_2)\phi_1-n_1\psi_{n_1}-n_2\psi_{n_2})$$
$$=(\lambda_{n_2}-\lambda_{n_1})\cot((n_2-n_1)\phi_2-n_2\psi_{n_2}+n_1\psi_{n_1})$$
$$+(\lambda_{n_2}+\lambda_{n_1})\tan((n_1+n_2)\phi_2-n_1\psi_{n_1}-n_2\psi_{n_2}). \tag{D10}$$

This can also be written as

$$\frac{[(\lambda_{n_2}-\lambda_{n_1})-(\lambda_{n_1}+\lambda_{n_2})\tan((n_2-n_1)\phi_2-n_2\psi_{n_2}+n_1\psi_{n_1})\tan((n_1+n_2)\phi_1-n_1\psi_{n_1}-n_2\psi_{n_2})]}{\tan((n_2-n_1)\phi_2-n_2\psi_{n_2}+n_1\psi_{n_1})}$$

$$-\frac{\begin{array}{l}[(\lambda_{n_2}-\lambda_{n_1})-(\lambda_{n_1}+\lambda_{n_2})\tan((n_2-n_1)\phi_1-n_2\psi_{n_2}\\ +n_1\psi_{n_1})\tan((n_1+n_2)\phi_2-n_1\psi_{n_1}-n_2\psi_{n_2})]\end{array}}{\tan((n_2-n_1)\phi_1-n_2\psi_{n_2}+n_1\psi_{n_1})}=0. \tag{D11}$$

Substitution of equation (C9) simplifies equation (D11) into

$$\left(\tan((n_1+n_2)\phi_1-n_1\psi_{n_1}-n_2\psi_{n_2})\tan((n_2-n_1)\phi_2-n_2\psi_{n_2}+n_1\psi_{n_1})-\frac{\lambda_{n_2}-\lambda_{n_1}}{\lambda_{n_2}+\lambda_{n_1}}\right)$$
$$\times(\tan((n_2-n_1)\phi_1-n_2\psi_{n_2}+n_1\psi_{n_1})-\tan((n_2-n_1)\phi_2-n_2\psi_{n_2}-n_1\psi_{n_1}))=0. \tag{D12}$$

APPENDIX E: DIMENSIONS AND MATERIAL PROPERTIES OF THE PERFECT RING (TABLE E1)

Mean radius = 0·3 m; Radial thickness = 0·005 m; Axial length = 0·1 m; Mass of ring = 7·3984 kg; Density = 7850 kg/m^3; Young's modulus = $2{\cdot}06\times10^{11}$ N/m^2; the Poisson ratio = 0·3.

TABLE E1

Natural frequencies and amplitude ratios

Nodal diameters, n_j	Natural frequency (Hz)	Amplitude ratio W/U
2	36·779	1·99992
3	104·026	2·99956
4	199·461	3·99877
5	322·571	4·99743
6	473·205	5·99540

APPENDIX F: NOMENCLATURE

a	ring cross-sectional area $= hL$
E	Young's modulus
h	ring radial thickness
K_{rp}	stiffness of pth radial ring
L	ring axial length
R	ring mean radius
β	$(= h^2/(12R^2))$
ρ	density of ring material
v	the Poisson ratio